Energetics of donor-doping, metal vacancies and oxygen-loss in A-site Rare-Earth doped $BaTiO_3$.

C.L. Freeman[1], J.A. Dawson[1], H.-R. Chen[1], L. Ben[1], J.H. Harding[1], F.D. Morrison[2], D.C. Sinclair[1] and A.R. West[1].

1. Department of Materials Science & Engineering, Sir Robert Hadfield Building, University of Sheffield, Mappin Street, Sheffield, S1 3JD, United Kingdom.

2. School of Chemistry, North Haugh, St Andrews University, Fife, KY16 9ST, United Kingdom.

Abstract

The energetics of La-doping in $BaTiO_3$ are reported for both (electronic) donor-doping with the creation of Ti^{3+} cations and ionic doping with the creation of Ti vacancies. Our experiments (for samples prepared in air) and simulations demonstrate that ionic doping is the preferred mechanism for all concentrations of La-doping. The apparent disagreement with electrical conduction of these ionic doped samples is explained by subsequent oxygen-loss which leads to the creation of Ti^{3+} cations. Our simulations show that oxygen-loss is much more favourable in the ionic-doped system than pure $BaTiO_3$ due to the unique local structure created around the defect site. These findings resolve the so-called 'donor-doping' anomaly in $BaTiO_3$ and explain the source of semiconductivity in positive temperature coefficient of resistance (PTCR) $BaTiO_3$ thermistors.

Trivalent rare earth (RE) ions are commonly used to modify the electrical properties of ferroelectric perovskite $BaTiO_3$ (ABO_3) ceramics in applications such as multi-layer ceramic capacitors (MLCC's) [1] and positive temperature coefficient of resistance (PTCR) thermistors [2]. Due to the intermediate size and charge of the RE^{3+} ions compared to the $Ba^{2+}$and Ti^{4+} ions, several aliovalent doping mechanisms (ionic and electronic) are plausible. In general, based on ion size effects, small RE^{3+} ions such as Yb^{3+} dope exclusively on the B-site with charge compensation by oxygen vacancies ($BaTi_{1-b}RE_bO_{3-b/2}$), intermediate sized RE^{3+} ions such as Gd^{3+} can dope simultaneously onto the A- and B-sites (so-called self compensation, $Ba_{1-a}RE_aTi_{1-b}RE_bO_3$) and large RE^{3+} ions such as La dope exclusively on the A-site [3]. In many cases, however, the doping mechanism(s) are also dependent on processing parameters such as the oxygen partial pressure (pO_2), sintering temperature/time and the overall A/B ratio in the formulation of the device [1]. The situation is further complicated as commercial devices are heterogeneous and deliberately prepared under non equilibrium conditions to optimise/control the desired electrical properties. For example, short sintering times are employed in MLCC's to ensure limited diffusion of dopants such as RE^{3+} ions into the grains to create so-called grain core-shell microstructures that are required to modify the temperature dependence of the permittivity and therefore capacitance of the device [1]. In the case of semiconducting PTCR-$BaTiO_3$ thermistors, low levels (<< 1 at%) of RE^{3+} doping occurs on the A-site and devices are cooled in air from the sintering temperature to allow limited (but necessary) up-take of oxygen along the grain boundaries. This is required to develop and/or enhance the Schottky barriers between the semiconducting grain-insulating grain boundary junctions to create such a non-ohmic device [2].

A-site doping of RE^{3+} ions has been a challenging topic for many years with the room temperature *dc* resistivity of ceramics being either semiconducting or insulating depending on the level of dopant and/or ceramic processing conditions [4-10]. A schematic diagram of the dc (total) resistivity of A-site doped RE^{3+}-$BaTiO_3$ ceramics processed in air at ~ 1400 ^oC is shown in Fig. 1. The resistivity decreases by > 8 orders of magnitude with low levels of doping (<< 1 at%) to yield semiconducting ceramics; however, the *dc* resistivity becomes insulating with higher doping levels (solid line, Fig. 1). A popular interpretation of this result for RE = La based

on *dc* conductivity experiments of ceramics [4-6, 11] and atomistic simulations of Lewis and Catlow [12] is that there is a switch in the doping mechanism with increasing doping level. At low dopant levels an electronic (donor doping) mechanism occurs to induce the semiconductivity but there is a switch to an ionic compensation mechanism at higher doping levels to re-establish the insulating behaviour [4-6]. The arrow in Fig. 1 indicates A-site RE^{3+} doping levels that are used on an industrial scale to produce PTCR thermistors (typically 0.2-0.5 at%). In recent years, we have questioned this interpretation of Fig. 1 and in particular, the need for a magic switch in the doping mechanism [13].

Due to its large size, La is unique as a RE^{3+} dopant in $BaTiO_3$ as it substitutes only on the A-site [7-10, 14, 15]; self-compensation and/or B-site doping do not occur. There are three plausible A-site doping mechanisms; 3 $Ba^{2+} \rightarrow 2\ La^{3+}$ with the creation of A-site vacancies ($Ba_{1-3x}La_{2x}TiO_3$); $Ba^{2+} + ¼\ Ti^{4+} \rightarrow La^{3+}$ with the creation of Ti-site vacancies ($Ba_{1-y}La_yTi_{1-y/4}O_3$); and, so-called donor-doping *via* the electronic compensation mechanism $Ba^{2+} \rightarrow La^{3+} + e^-$ ($Ba_{1-z}La_zTiO_3$). Several experimental phase diagram studies for samples prepared in air according to the various A-site compensation mechanisms have all shown the favoured mechanism to be the creation of Ti-site vacancies ($V_{Ti}^{////}$) with an extensive solid solution limit of y ~ 0.20 – 0.25 [10,14,15]. There is no experimental evidence for the existence of the Ba-vacancy or donor-doping mechanism(s), at least down to the detection limits of the techniques employed in the reported phase-diagram studies, i.e. X-ray diffraction and analytical electron microscopy. Samples prepared according to the donor-doping mechanism give phase mixtures of $Ba_{1-y}La_yTi_{1-y/4}O_3$ and other Ti-rich phase(s) such as $Ba_6Ti_{17}O_{40}$ [8]. Due to the immobility of metal vacancies at ambient conditions all $Ba_{1-y}La_yTi_{1-y/4}O_3$ prepared in air are expected to be room temperature electrical insulators.*

**Footnote: It is noteworthy that recent Density Functional Theory (DFT) studies on La-doped BT [16] observed exclusive doping on the A-site with a variation in the compensation mechanism between electronic compensation for reducing atmospheres, eg 5 % H_2, and Ti vacancies for Ba-rich and oxidising atmospheres. This suggests the locus of the solid solution in the phase diagram will be different for samples prepared in air compared to 5 % H_2. To our knowledge, an analogous experimental study has not been conducted.*

The problem, however, is that the electrical properties of La-doped $BaTiO_3$ ceramics (and that of other A-site RE^{3+} doped materials such as Gd, Ho, Dy) are very dependent on the processing conditions such as the oxygen partial pressure, the sintering temperature and the rate of cooling from the sintering temperature. For example, sintering (and subsequent cooling) all single-phase $Ba_{1-y}La_yTi_{1-y/4}O_3$ compositions at 1400 ºC in flowing oxygen results in electrically homogeneous ceramics. Impedance Spectroscopy (IS) reveals the grain and grain boundary regions to be electrically insulating ($> 10^8$ Ωcm) at room temperature irrespective of y and there is no anomaly between the doping mechanism observed by the equilibrium phase diagram studies and the measured electrical properties [9]. Sintering (and subsequent cooling) all single-phase $Ba_{1-y}La_yTi_{1-y/4}O_3$ samples at 1400 ºC in air, however, results in electrically heterogeneous ceramics [9,10,13]. IS reveals two extreme types of electrical microstructures that are dependent on y and/or the ceramic microstructure of the ceramics [9]. In some cases, usually for small values of y (<< 0.01), the grains are semiconducting and the grain boundaries are insulating and this can give rise to the very useful PTCR effect for thermistor applications, see arrow in Fig. 1. In other cases, usually for larger values of y (> 0.01), the outer regions (skin or surface layer) of the ceramic is electrically insulating at room temperature whereas the inner regions (core) of the ceramic remain semiconducting. In all cases, the samples remained single phase but IS reveals the room temperature grain resistivity to vary from ~ 10 to $>10^8$ Ωcm for the same value of y depending on the processing atmosphere (air or oxygen, respectively) or the region of the ceramic studied (inner or outer regions, respectively). It is clear, therefore, that thermodynamics and kinetics can both play an important role in shaping the electrical properties of these materials.

These results led us to conclude that (electronic) donor-doping of $BaTiO_3$ with La (or any other trivalent RE^{3+} doped on the A-site) was not a feasible doping mechanism for samples prepared in air and was not the source of the semiconductivity [13]. Instead, we proposed the favoured doping mechanism to be the creation of Ti vacancies, i.e. $Ba_{1-y}La_yTi_{1-y/4}O_3$ and the source of semiconductivity to be the loss of a small amount of oxygen that occurs when sintering such compositions in air at high temperatures, i.e.

$$O^{2-} \rightarrow \tfrac{1}{2}\, O_2\,(g) + 2\, e^- \qquad (1)$$

with the electrons being transferred to partially reduce some of the Ti^{4+} (d^0) to Ti^{3+} (d^1) ions [13]. The general formula could therefore be written as $Ba_{1-y}La_yTi_{1-y/4}O_{3-\delta}$ where δ represents the oxygen loss. Based on the equation for conductivity, $\sigma = nq\mu$, with the lowest room temperature grain core resistivity of ~ 10 Ωcm (see shaded box with dashed line in Fig. 1) and a mobility (μ) value of ~ 0.1 – 1.0 $cm^2/(Vs)^2$ [5, 17, 19] for $BaTiO_3$, the carrier concentration (n) can be estimated to be ~ 6 x 10^{16} to 6 x 10^{17} cm^{-3} independent of y. This puts an upper limit on δ to be ~ 0.0002. The observed electrical properties obtained for single-phase La-doped ceramics therefore depend on the sintering atmosphere, the cooling rate and the ceramic microstructure as this dictates the level and distribution of oxygen up-take on cooling. It should be noted that oxygen-loss is well known to induce semiconductivity in un-doped $BaTiO_3$ when processed in inert or reducing atmospheres at temperatures above ~ 1200 ^oC [5].

Our model to explain Fig. 1 was still perceived to be controversial, especially as existing classical simulations by Buscaglia *et* al [20] using a potential developed by Lewis and Catlow [12] suggested donor doping of La to be the lowest energy doping mechanism, at least for low levels of doping. Also, why should La-doping on the A-site facilitate oxygen-loss for samples prepared in air at > 1200 ^oC? Prediction of the exact doping mechanisms and defect structures in doped $BaTiO_3$ is desirable and although a recent DFT study [16] was in agreement with our experimental phase diagram for samples prepared in air and/or flowing O_2 gas the cost of DFT simulations to study possible defect clusters and their segregation is prohibitively expensive.

The Lewis and Catlow model [12] was developed in the mid 1980s and was a completely ionic model. The origin of ferroelectricity in $BaTiO_3$ depends on the occurrence of covalency in the bonding between the Ti and O atoms. We have recently developed a new potential model for $BaTiO_3$ [21] to account for this covalency which has resulted in much better agreement between experimental and calculated values for the lattice parameters and cohesive energy of $BaTiO_3$. See [21] for more details on the model and a general discussion of the results for RE-doping in $BaTiO_3$. A key result from this new model is the prohibitively large solution energy of all RE donor-doping compared to that reported by the Lewis and Catlow model [12]. For La-doping, our model predicts 9.06 eV compared to 0.22 eV based on the Lewis and Catlow model, Table I (a). The solution energy of 1.01 eV for the Ti-vacancy (ionic) compensation mechanism for La at infinite dilution is much more favourable compared with 9.06 eV for donor-doping

(electronic) compensation in this new model, Table I (a). Calculations have also been performed for y (ionic compensation) and z (electronic compensation) = 0.04, 0.08 and 0.12 (rows 3 and 7 in Table I (b), respectively) and in every case the solution energy is always considerably lower for the Ti-vacancy mechanism. This result is in excellent agreement with the equilibrium phase diagram of La_2O_3-BaO-TiO_2 for samples prepared in air and/or flowing oxygen and with a DFT study [16]. It is also in agreement with the insulating electrical properties of $Ba_{1-y}La_yTi_{1-y/4}O_3$ ceramics processed in flowing oxygen [9,10].

To explain the electrical properties of $Ba_{1-y}La_yTi_{1-y/4}O_3$ ceramics prepared in air, calculations were performed that considered the solution energy for the creation of oxygen vacancies associated with oxygen loss from both pure $BaTiO_3$ and doped $Ba_{1-y}La_yTi_{1-y/4}O_3$ to form semiconducting $Ba_{1-y}La_yTi_{1-y/4}O_{3-\delta}$ in the latter case. Static lattice minimisation calculations were all performed with the GULP 3.1 code [22]. The defect energies were calculated using the Mott-Littleton two region approach [23]. Several potential defect clusters were attempted and the lowest energy arrangement is reported. For the calculation of defect effects in y = 0.04, 0.08 and 0.12 a 100 formula unit cell was used. The range of potential defect clusters was sampled using four separate genetic algorithm (GA) runs on a group of twenty random starting populations of defect sites. The selectivity of breeding between successful populations was set at 50% and forty breeding rounds were attempted. The mutation rate was set at 10%. To reduce computational expense initial runs calculated only the single point energy of the cell. From these results twenty new populations were selected for four further GA runs using the same conditions, but now allowing for full optimisation of the cell, were performed.

The calculations show ~ 6.63 – 8.61 eV is required to release oxygen from the undoped $BaTiO_3$ lattice to form $V_O^{\bullet\bullet}$ + 2 $Ti_{Ti}^{/}$ (row 4, Table I (b)). This energy is significantly reduced when oxygen loss is considered in the presence of the RE^{3+} defect cluster with binding energies of the oxygen vacancy cluster and RE^{3+} cluster of ~ -4.29 to -7.00 eV (row 6, Table I (b)). This clearly shows the overall energy associated with the oxygen-loss model (row 5, Table I (b)) is substantially lower when compared to direct donor doping of La (row 7, Table I (b)) and confirms this model as the source of semiconductivity in $Ba_{1-y}La_yTi_{1-y/4}O_3$ ceramics prepared in air at high temperatures.

Oxygen loss is energetically favoured at the La-defect cluster due to the particular local structure for $Ba_{0.96}La_{0.04}Ti_{0.99}O_{3-\delta}$ (y =0.04) that is shown in Fig. 2. The lowest energy arrangement of the defects is with the $V_O^{\bullet\bullet}$ occurring adjacent to the $V_{Ti}^{////}$ and surrounded by Ba^{2+} A-site cations only, Fig. 2 (a). The loss of the Ti reduces the local Madelung potential in the surrounding oxygen anions. Although the presence of the $La_{Ba}^{\bullet}$ with a 3+ charge on each La will increase the potential for the oxygen anions that nearest neighbour to these cations (labelled 1 to 5 in Fig. 2(b)) but for the single oxygen anion further away (labelled 6 in Fig. 2 (b)) the potential will be significantly diminished. Therefore there is a smaller energy penalty for this oxygen to exit the lattice compared to other oxygen anions. The electron compensation this causes within the lattice generates two Ti^{3+} ions ($Ti_{Ti}^{/}$). The first $Ti_{Ti}^{/}$ is naturally preferred next to the $V_O^{\bullet\bullet}$ due to the Coulomb attraction of the charged defect sites. The most favourable position of the second $Ti_{Ti}^{/}$ is adjacent to the four $La_{Ba}^{\bullet}$ as the reduction of the Ti here from 4+ to 3+ reduces the Coulombic repulsion between the cations.

Millions of PTCR $BaTiO_3$ thermistors are produced annually for a wide variety of applications. Since the late 1960's, it has been widely accepted that the A-site RE^{3+} doping required to produce semiconducting grains originates from direct donor-doping. The calculations presented here and in combination with previous experimental results [7-10,13] show this to be incorrect. Instead, the formation of titanium vacancies and the arrangement of the RE^{3+} ions on the A-sites facilitate a mechanism for removal of oxygen anions from the lattice and this is the source of the semiconductivity for samples processed under the conditions commonly employed to manufacture PTCR $BaTiO_3$ thermistors.

We thank the EPSRC (EP/G005001/1) for funding. CLF would like to thank EPSRC grants (EP/I016589/1) and (EP/I001514/1) for additional funding.

References

[1] H. Kishi, Y. Mizuno and H. Chazono, Jpn. J. Appl. Phys. Part 1 **42,** 1 (2003)

[2] W. Heywang, Solid State Electron. **3**, 51 (1961).

[3] Y. Tsur, T.D. Dunbar and C.A. Randall, J. Electroceram. **7**, 25 (2001).

[4] C.J. Peng and H.-Y. Lu, J. Am. Ceram. Soc. **71**, C44 (1988)

[5] J. Daniels, K.H. Hardtl, D. Hennings and R. Wernicke, Philips Res. Rep. **31**, 487 (1976).

[6] N.-H. Chan and D.M. Smyth, J. Am. Ceram. Soc. **67**, 285 (1984).

[7] F.D. Morrison, D.C. Sinclair, J.M.S. Skakle and A.R. West, J. Am. Ceram. Soc. **81**, 1957 (1998).

[8] F.D. Morrison, D.C. Sinclair and A.R. West, J. Appl. Phys. **86**, 6355 (1999).

[9] F.D. Morrison, D.C. Sinclair and A.R. West, J. Am. Ceram. Soc. **84**, 531 (2001).

[10] F.D. Morrison, A.M. Coats, D.C. Sinclair and A.R. West, J. Electroceram. **6**, 219 (2001).

[11] D.M. Smyth, J. Electroceram. **9**, 179 (2002).

[12] G.V. Lewis and C.R.A. Catlow, J. Phys. Chem. Solids **47**, 89 (1986).

[13] F.D. Morrison, D.C. Sinclair and A.R. West, J. Am. Ceram. Soc. **84**, 474 (2001).

[14] G.H. Jonker and E.E. Havinga, Mater. Res. Bull. **17**, 345 (1982).

[15] D. Makovec, Z. Samrdzija, U. Delalut and D. Kolar, J. Am. Ceram. Soc. **78**, 2193 (1995).

[16] H. Moriwake, C.A.Fisher and A. Kuwabara, Jpn. J. Appl. Phys. **48**, 09KC03 (2009).

[17] A.M.J.H. Seuter, Philips Res. Rep. Suppl. **31**, 487 (1976).

[18] J. Nowotny and M. Rekas, Ceram. Int. **20**, 237 (1994).

[19] C.-R. Song and H.-I. Yoon, Phys. Rev. **B61**, 3975 (2000).

[20] M. Buscaglia, V. Buscaglia, M. Viviani and P. Nanni, J. Am. Ceram. Soc. **84**, 376 (2001).

[21] C.L. Freeman, J.A. Dawson, H.-R. Chen, J.H. Harding, L.-B. Ben and D.C. Sinclair, J. Mater. Chem. **21**, 4861 (2011).

[22] J. Gale and A. Rohl, Mol. Simul. **29**, 291 (2003).

[23] M. Mott and M. Littleton, Trans. Faraday Soc. **34**, 0485 (1938).

Table I. (a) Solution energies for electronic ($e^{/}$) and ionic ($V_{Ti}^{////}$) doping mechanisms in La-doped $BaTiO_3$ based on models by Lewis and Catlow [12] and Freeman *et al* [21]. (b) Solution energies for the electronic ($e^{/}$) and ionic ($V_{Ti}^{////}$) doping mechanisms in La-doped $BaTiO_3$ with 0.00 (infinite dilution), 0.04, 0.08 and 0.12 mole fraction of La^{3+} on the A-site. Also shown are the energies of oxygen-loss and the creation of 2 Ti^{3+} from the freed $e^{/}$ in the pure $BaTiO_3$ lattice and in the presence of the ionic defect cluster. The binding energy of the oxygen vacancy and the La defect cluster is listed where a negative value indicates a preferred binding in the lattice. The energies for the defects with y = 0.04, 0.08 and 0.12 are calculated for the whole cluster, i.e. for all 4, 8 or 12 La^{+} ions. The energies for the infinitely dilute case at y = 0.00 are calculated per La^{3+} ion.

(a)	$La_{Ba}^{\bullet} + e^{/}$		$4\ La_{Ba}^{\bullet} + V_{Ti}^{////}$	
	Lewis & Catlow [12] (eV)	Freeman *et al* [21] (eV)	Lewis & Catlow [12] (eV)	Freeman *et al* [21] (eV)
Solution Energies	0.22[(a)]	9.06	2.90[(a)]	1.01

(a) Taken from [20]

(b)	Mole fraction of La^{3+} on A-site			
	0 %[(b)] (eV)	4 % (eV)	8 % (eV)	12 % (eV)
$4xLa_{Ba}^{\bullet} + V_{Ti}^{////}$	1.01	4.44	9.15	13.0
$2xTi_{Ti}^{/} + V_O^{\bullet\bullet}$	6.63	8.61	8.61	8.61
$4xLa_{Ba}^{\bullet} + V_{Ti}^{////} + 2xTi_{Ti}^{/} + V_O^{\bullet\bullet}$	3.23	9.68	10.73	14.61
Binding Energy	-4.29	-3.37	-7.03	-7.00
$4x(La_{Ba}^{\bullet} + e)^{/}$	9.06	12.24	24.44	36.98

(b) 0% refers to isolated defect calculations so the defects are at an infinite dilution.

Figure 1. Schematic diagram showing the variation in *dc* resistivity of La-doped $BaTiO_3$ ceramics processed in air at 1400 ^{O}C followed by rapid cooling to room temperature (solid black line). Dashed and vertically shaded (yellow/green) box indicates the range of the lowest grain core resistivity values obtained from Impedance Spectroscopy. The range of compositions suitable for PTCR thermistors is indicated by the horizontally shaded (yellow/purple) box.

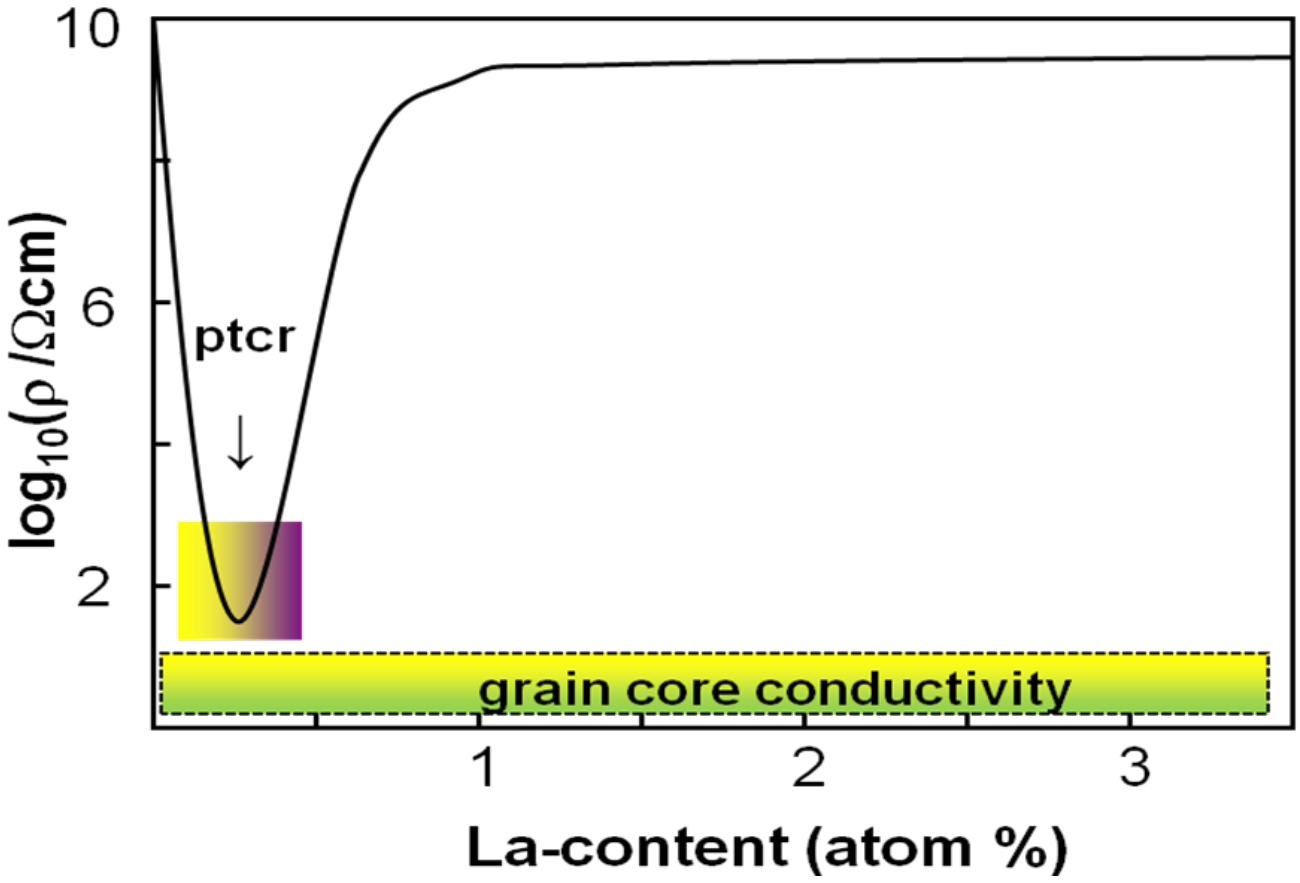

Figure 2. (a) The relaxed structure of the defect sites in 4% La-doped $BaTiO_3$ by ionic compensation with 4 La_{Ba} and Ti vacancies coupled with O loss to create Ti^{3+} ions. Key: oxygen (red); titanium (purple); barium (silver); lanthanum (blue); Ti^{3+} (green); V_O (circle with cross); V_{Ti} (circle with dot). (b) Schematic diagram to show the removal of O(6) from $Ba_{1-y}La_yTi_{1-y/4}O_3$.